HHS Public Access

Author manuscript

Virology. Author manuscript; available in PMC 2019 September 01.

Published in final edited form as:

Virology. 2018 September ; 522: 92–105. doi:10.1016/j.virol.2018.07.008.

Murine cytomegalovirus M72 promotes acute virus replication *in vivo* and is a substrate of the TRiC/CCT complex

Sandhya Gopal[a], **Encarnacion Perez Jr.**[a], **Amanda Y. Xia**[a], **Jonathan J. Knowlton**[b], **Filipe Cerqueira**[a], **Terence S. Dermody**[b,c], and **Jason W. Upton**[a,*]

[a]Department of Molecular Biosciences, LaMontagne Center for Infectious Disease, Institute for Cellular and Molecular Biology, University of Texas at Austin, 100 E. 24th Street Stop A5000, Austin, TX 78712, USA

[b]Department of Pediatrics, University of Pittsburgh School of Medicine, Pittsburgh, PA, USA

[c]Department of Microbiology and Molecular Genetics, University of Pittsburgh School of Medicine, Pittsburgh, PA, USA

Abstract

Betaherpesvirus dUTPase homologs are core herpesvirus proteins, but little is known about their role during infection. Human cytomegalovirus (HCMV) UL72 and murine cytomegalovirus (MCMV) M72 have been designated dUTPase homologs, and previous studies indicate UL72 is dispensable for replication and enzymatically inactive. Here, we report the initial characterization of MCMV M72. M72 does not possess dUTPase activity, and is expressed as a leaky-late gene product with multiple protein isoforms. Importantly, M72 augments MCMV replication *in vitro* and during the early stage of acute infection *in vivo*. We identify and confirm interaction of M72 with the eukaryotic chaperonin tailless complex protein −1 (TCP-1) ring complex (TRiC) or chaperonin containing tailless complex polypeptide 1 (CCT). Accumulating biochemical evidence indicates M72 forms homo-oligomers and is a substrate of TRiC/CCT. Taken together, we provide the first evidence of M72's contribution to viral pathogenesis, and identify a novel interaction with the TRiC/CCT complex.

Keywords

Herpesvirus; Cytomegalovirus; Murine cytomegalovirus; MCMV; Pathogenesis; DUTPase; TRiC/CCT

1. Introduction

Human cytomegalovirus (HCMV), a betaherpesvirus, is the major infectious cause of birth defects in developed countries (Griffiths, 2012). It has the potential to cause permanent neurological damage including microcephaly, cognitive impairment and sensorineural

*Corresponding author. upton@austin.utexas.edu (J.W. Upton).

Conflict of interest

Authors declare that they have no conflicts of interest.

hearing loss in CMV-infected newborns (Boppana et al., 2013). Owing to the high cost of caring for children with congenital CMV infection, it has been prioritized as a candidate for vaccine development in the United States (Stratton et al., 2000). Immunocompromised individuals, including transplant recipients and HIV-infected persons, represent another susceptible population where HCMV represents a major cause of morbidity and mortality. In this group, problems arise due to acute infection or reactivation and include retinitis, hepatitis, and pneumonitis (Plosa et al., 2012; Ramanan and Razonable, 2013).

The narrow host range of HCMV makes it challenging to study the role of viral genes in the context of natural host. Hence, murine CMV (MCMV) infections of mice are used as a tractable animal model for studies of CMV pathogenesis. Sequence and functional homologs of viral genes among the CMVs of different hosts facilitate studies of specific pathogenic mechanisms (Barry et al., 2006; Schleiss, 2006). MCMV has a wide variety of genes that contribute to its ability to infect and evade the host responses. This leads to the establishment of an intricate life-long host pathogen relation, characteristic of all herpesviruses. The gamut of MCMV genes includes a subset of core genes that are evolutionarily conserved across herpesviruses. Most of these genes encode proteins required for replication and virus structure. However, many core genes remain relatively uncharacterized, and little is known about their contribution to infection. The MCMV gene, M72, designated as a 2′ deoxyuridine 5′triphosphate pyrophosphatase (dUTPase) homolog, is one such example of a core gene with no identified function (Mocarski Jr, 2007).

Cellular dUTPases are ubiquitous enzymes that convert dUTP to dUMP and pyrophosphate (PPi) to control cellular nucleotide pools and prevent misincorporation of uracil into cellular DNA. There are several examples of viral dUTPases among retroviruses and DNA viruses (Baldo and McClure, 1999). The dUTPase-encoding gene in non-primate lentiviruses is essential for replication in non-dividing cells (Hizi and Herzig, 2015). Similarly, a feline immunodeficiency virus (FIV) dUTPase mutant displays a reduced viral burden *in vivo*, suggesting a contribution to infection in the natural host (Lerner et al., 1995). Among herpesviruses, a dUTPase-encoding gene is present in all three herpesvirus family subdivisions, and the alpha- and gamma-herpesviruses dUTPases are functional enzymes (Davison and Stow, 2005). The varicella zoster virus (VZV) and simian varicella virus (SVV) dUTPases, encoded by ORF8 of each virus, contribute to virus replication in cell culture (Ross et al., 1997; Ward et al., 2009). Additionally, a herpes simplex virus (HSV) 1 dUTPase, UL50, null mutant is less virulent compared to wild type virus and exhibits decreased neurovirulence (Pyles et al., 1992).

Many herpesvirus dUTPases have functions independent of their dUTPase activity. Kaposi's sarcoma-associated herpesvirus (KSHV) and murid herpesvirus-68 (MHV-68) ORF54 down-regulate a cell-surface ligand, NKp44L (Madrid and Ganem, 2012), and degrade IFN receptor 1 protein (Leang et al., 2011), respectively. EBV dUTPase, BLLF3, activates NF-κB (Ariza et al., 2009) and induces the secretion of pro-inflammatory cytokines in a TLR2-dependent manner (Ariza et al., 2013). Thus, there are functions associated with alpha- and gammaherpesvirus designated dUTPases independent of their catalytic activity.

Little is known about the betaherpesvirus dUTPase homologs. Preliminary characterization of the HCMV designated dUTPase homolog, UL72, revealed it to be catalytically inactive and dispensable for replication in cell culture (Caposio et al., 2004). Here, we report that the MCMV designated dUTPase homolog, M72, is also non-functional as a dUTPase enzyme, augments virus replication in some cell types and contributes to viral pathogenesis in the acute phase of replication in the natural host. We also find that the M72 protein is expressed from early times post infection, shows a complex expression profile that includes multiple shorter isoforms, and is a substrate of the eukaryotic chaperonin tailless complex protein −1 (TCP-1) ring complex (TRiC)/chaperonin containing tailless complex polypeptide 1 (CCT). Together, this initial characterization of M72 reveals new insight into betaherpesvirus dUTPases homologs and highlights the contribution of M72 to viral pathogenesis.

2. Materials and methods

2.1. Plasmids and transfections

M72 expression constructs were generated by PCR amplification of nucleotides 104,289 to 103,084 using MCMV K181 bacterial artificial chromosome (BAC) pARK25 (Accession No. AM886412.1) (Redwood et al., 2005), as template. Amplicons were cloned into the *EcoRI* and *XbaI* sites of p3XFLAG-CMV10 or p3XFLAG-CMV14 expression constructs (Sigma-Aldrich) or the *EcoRI* and *KpnI* sites of pEGFP-C1 (Clontech). Transfections were performed using GenJet transfection reagent (SignaGen Laboratories) according to manufacturer instructions. HA-CCT expression constructs (Kim et al., 2014) were a kind gift from Dr. Kyong-Tai Kim (Pohang University of Science and Technology, Republic of Korea). FLAG-tagged MHV68 ORF54 and ORF54$^{H80A/D85N}$ expression constructs (Leang et al., 2011) were a kind gift from Drs. Ting-Ting Wu and Ren Sun (University of California at Los Angeles).

2.2. Cells and reagents

STO (CRL-1503), HEK293Ts (ATCC CRL-3216), SVEC4–10 endothelial cells (ATCC CRL-2181) and RAW264.7 murine macrophages (ATCC TIB-71) were propagated in Dulbecco's modified Eagle's medium (DMEM – Sigma-Aldrich) containing 10% heat-inactivated fetal calf serum (FCS, Life Technologies, Inc.) and 1% penicillin-streptomycin-glutamine (PSG, Life Technologies, Inc.). NIH3T3 murine fibroblasts (ATCC CRL-1658) were propagated in DMEM containing 10% heat-inactivated bovine calf serum (BCS, Life Technologies) and 1% PSG. Bone marrow-derived macrophage (BMDM) cultures were generated as previously described (Kaiser et al., 2013). Briefly, pooled bone marrow cells from flushed tibias and femurs were harvested into Dulbecco's PBS, placed in culture for at least 18 h in DMEM containing 10% FBS, and then differentiated for 5–7 days in DMEM containing 20% FBS and 20% L929-conditioned medium. Phosphonoformic acid (PFA) was from Sigma-Aldrich.

2.3. Generation of recombinant viruses

BAC mutagenesis and diagnosis was performed by recombineering as previously described (Upton et al., 2010). Briefly, *E. coli* DH10B cells containing pARK25 and pSIM6 (Datta et al., 2006) were grown to O.D.600 of 0.4–0.6, recombination functions induced by

incubation at 42 °C and cells made electrocompetent by multiple washes in ice cold water. The levansucrase (SacB) and kanamycin (Kan) genes were amplified from plasmid pTBE100 (Upton et al., 2010) with 60 nucleotide base pair overhangs corresponding to MCMV genomic sequences. PCR reactions were treated with *DpnI*, and amplicons gel purified then used to electroporate induced bacteria. Kanamycin-resistant, sucrose-sensitive clones were selected and assessed for insertion and genomic integrity by PCR and RFLP analysis. M72.SK (primers; SG005, 5′-*ACGG GACGCCTGCACAACGTCGGAAGGCGTCGCGACCTCGAGGAACAAAAG CAGCAGCAC*AATTCGAGCTCGGTACCCGG-3′ and SG006, 5′-*ATCACG ATCTTGTTGACGGTCGTATCCGGCACCGAAGCGGCGACCGACACCGGT ACGGAGGCC*ATCCCGGGAAAAGTGCCACC-3′: italic indicates viral sequence) deletes viral sequence between nucleotide 102,772 – 105,791 and M72Flag.SK (primers; FC001, 5′*GGTAAACGTAGTTTTCCTGAGTA CACTAGACAAGAGGTAATCTCTCTAGG*AATTCGAGCTCGGTACCCGG-3′ and FC002, 5′-*ACCGCGCGGAAGAGAGAATGCGAAGCGGTCG AGACTCGTCGAACGAGGGC*ATCCCGGGAAAAGTGCCACC) deletes the M72 stop codon (nucleotides 103,083 – 103,086) and introduces an additional 2.9Kb of sequence. Specific mutations were introduced by a second round of recombineering with individual amplicons generated by overlap extension PCR. M72StopS (primers; SG007, 5′-ATGAAGGA TCCCTTTAATATCTTCGAC**TA**<u>**GT**</u>ACGAACCTTCC-3′ and SG015, 5′-GGAAGGTTCGT<u>A**CT**</u>**A**GTCGAAGATATTAAAGGGATCCTTCAT 3′; bold indicates nucleotide substitution, underline indicates diagnostic restriction enzyme recognition site) and M72StopN (primers; SG009, 5′-ATGAAGGATCCCTTTAATA<u>**G**CT**AGC**</u>ACGACGACGAACCTTCC-3′ and SG016, 5′-GGAAGGTTCGTCGTCGT<u>**GCT**AG**C**</u>TATTAAAGGGATCCTTCAT-3′) contain an engineered stop codon and a *SpeI* (nt 104,124 – 104,127), or an *NheI* (nt 104,135–104,130) diagnostic restriction site, respectively. M72.3XFlag inserts three tandem FLAG epitopes at the C-terminal end of M72, and was constructed by recombineering with an amplicon generated by overlap extension PCR (primers; FC003, 5′-GGACGTGTAAGTGTGTGGATTGTTG-3′ and FC009, 5′-TGACCTAGA GAGATTACCTCTTGTCTAG using template pARK25; FC004, 5′- GATG GCCAAGATCATCTTCACGAC-3′ and FC010, 5′- CTAGACAAGAGGTAA TCTCTCTAGGTCACTACTTGTCATCGTCATCCTTGTAG-3′ template p3XFLAG-CMV-14-M72). Colonies were screened for kanamycin sensitivity and sucrose resistance, and positive clones confirmed by PCR and RFLP analysis. PCR amplification and diagnostic restriction digest of M72 region confirmed the incorporation of the mutagenesis in the M72 mutants. Infectious virus was reconstituted as previously described (Upton et al., 2010), amplified by growth in STO cells in the presence of 25 μg/ml 6-thioguanine (Sigma-Aldrich, St. Louis, MO), and plaque purified by limiting dilution. Parallel stocks were produced by infecting BALB/cJ mice with initial transfection supernatants of WT and M72Stop mutants (M72StopS and M72StopN). Infected salivary glands were harvested 14 days post infection (d.p.i.), sonicated, clarified and used to infect NIH3T3 fibroblasts. Viral stocks were generated, clarified, concentrated and titered by plaque assay as previously described on NIH3T3 fibroblasts (Upton et al., 2010). All viral stocks were confirmed to be GFP

negative, indicating excision of the BAC. All M72 viral stocks were confirmed by sequencing of the recombineering junctions, introduced mutations, and surrounding regions.

2.4. Infections, in vitro growth, and determination of viral titers

Viral titers were determined by plaque assays performed on NIH3T3 fibroblasts. Viral growth *in vitro* was determined by infection of indicated cell lines at a multiplicity of infection (MOI) of 5 PFU per cell to measure single step growth kinetics, or at 0.05 PFU per cell to measure multiple cycles of replication. Viruses were adsorbed for 2 h. at 37 °C in a volume of 0.4 ml. Cells and supernatants for quantitation were harvested at indicated times post infection, and frozen at −80 °C. Samples were subjected to one round of freeze/thaw, and virus quantitated by plaque assay on NIH3T3 fibroblasts as previously described (Upton et al., 2010). Organs for virus quantitation were thawed and homogenized by sonication. Organ homogenates were serially diluted in complete media, and the titers were determined by plaque assay on NIH3T3 fibroblasts as previously described (Upton et al., 2010).

2.5. Immunoblotting

NIH3T3 fibroblasts were seeded in 35 mm dishes and infected with MCMV-M72.3XFlag recombinant virus at MOI of 5 PFU/cell in the absence or presence of 200 μg/ml Phosphonoformic acid (PFA, Sigma). Whole cell lysates were made at the indicated time points by removing media, washing the cells with PBS, adding 200 μl of 1× SDS-lysis buffer directly on the cells and freezing the dish at −20 °C. All the samples were heated at 95 °C for 10 min, run on 10% SDS-PAGE gel, immobilized on nitrocellulose membrane and probed with indicated antibodies.

2.6. Immunoprecipitation, immunoblotting and antibodies

Immunoprecipitations were performed by lysing transfected or infected cells in NP-40 lysis buffer (50 mM Tris pH 8.0, 150 mM NaCl, and 1% NP-40, supplemented with c0mplete Mini EDTA free Protease inhibitor cocktail (Roche), Phosphatase inhibitor cocktails 2 and 3 (Sigma-Aldrich)), incubating on ice for 20 min, and clarifying by highspeed centrifugation for 10 min. Supernatants were pre-cleared with Mouse IgG Agarose beads (Sigma), immunoprecipitated using anti-FLAG M2 affinity beads (Sigma), followed by elution with 20 μg of 3× FLAG peptide (Sigma). Samples were mixed with 2× - SDS sample buffer, boiled at 95 °C for 10 min, and resolved on 10% SDS-PAGE gels. Immunoblotting was performed as previously described (Upton et al., 2010). The following antibodies were used: mouse anti-FLAG M2-Peroxidase (Clone M2; Sigma-Aldrich), mouse anti-HA-peroxidase (Clone HA-7; Sigma-Aldrich), mouse anti-β-Actin (Clone AC-74; Sigma), mouse anti-m123/IE1 (CROMA101; Center for Proteomics, University of Rijeka), mouse anti-M112–113/E1 (CROMA103; Center for Proteomics, University of Rijeka), mouse anti-M55 (C1 M55.01; Center for Proteomics, University of Rijeka), rabbit anti-M86 (MCP – a gift from Laura Hanson, Texas Women's College, Denton, TX), rabbit anti-TCP1/CCT1 polyclonal (10320–1-AP, Proteintech), rabbit anti-CCT7 polyclonal (15994–1-AP, Proteintech), rabbit anti-CCT8 polyclonal (12263–1-AP, Proteintech), mouse anti-GAPDH-HRP (G9295, Sigma), donkey anti-mouse IgG-HRP (Vector Laboratories), and goat anti-rabbit IgG-HRP (Vector Laboratories). Blots were visualized using ECL Prime Western Blotting Detection Reagent (GE Healthcare) and exposed to film. Digital images were generated with a

CanoSCAN LIDE 700F slide/film scanner (Cannon) and images processed with Canvas X16 software (ACD Systems International, Ft. Lauderdale, DL, USA). No digital enhancements were applied.

2.7. Animal infections and organ harvest

BALB/cJ mice were obtained from the Jackson Laboratory. Animals were bred and maintained at the Animal Resources Center (ARC) at the University of Texas at Austin in accordance with the institutional guidelines. Male and female animals were used between 7 and 12 weeks of age. Intraperitoneal (i.p.) infections were performed by injection of 10^5 PFU in a volume of 0.5 ml. Upon sacrifice, organs were harvested by sterile dissection, placed into 1 ml complete DMEM and frozen at −80 °C before titer determination. Each time point represents n = 10 or 15 mice per group. All procedures were approved by the University of Texas at Austin Institutional Animal Care and Use Committee.

2.8. dUTPase assay

dUTPase assays were performed as previously described (Leang et al., 2011). Briefly, epitope tagged M72, MHV68 ORF54 or its catalytic mutant ORF54$^{H80A/D85N}$ were transfected into HEK293Ts. Cells were lysed 36 h post transfection in NP-40 lysis buffer on ice for 20 min, and clarified by centrifugation. Supernatants were pre-cleared with Mouse IgG Agarose beads (Sigma), immunoprecipitated using anti-FLAG M2 affinity beads (Sigma), followed by elution with 20 μg of 3× FLAG peptide (Sigma). 5 μl of purified FLAG-tagged proteins were incubated for indicated times at 37 °C with 5 μl of 5 mM dUTP (Promega) in 10 μl of 2× reaction buffer (100 mM Tris pH 7.5, 20 mM $MgCl_2$, 20 mM DTT, 0.2 mg/ml BSA). Reactions were terminated by freezing. PCR was performed using the dUTP sample, along with dATP, dCTP, and dGTP to amplify a small region of M72 expression plasmid DNA (primers; SG020 5′-CTTGAATTCAGCCACCATGGCGAAGCACAACAGA AGG-3′ and SG032, 5′-CAATCTAGACTTCTCGGGACGACGCGCTTCC-3′). PCR cycle conditions were 95 °C, 2 min; 94 °C, 30 s; 65 °C, 30 s; 72 °C, 30 s for 35 cycles, 72 °C 10 min and hold at 4 °C. PCR products were run on 2% agarose gel.

2.9. Sample preparation, LC/MS-MS, and data analysis

M72–3XFLAG or its corresponding empty vector control p3XFLAG-CMV-14 were transfected into NIH3T3 fibroblasts in 10 cm dishes. Whole cell lysates were collected 24 h later in 1% NP-40 lysis buffer and subjected to FLAG-immunoprecipitation as described above. Samples were eluted using 50 μg 3× FLAG peptide (Sigma) for 30 min on an orbital rotator at room temperature. Eluted proteins were boiled in 1× SDS sample buffer, separated on a 10% SDS-PAGE gel, stained with 0.1% Coomassie-Blue dye and destained. Bands present in the M72–3XFLAG lane compared to the vector control were selected, and gel slices submitted for liquid chromatography-tandem mass spectrometry (LC-MS/MS) analysis (Proteomics Core Facility, UT Austin). Gel bands were subjected to in-gel tryptic digest and separated by liquid chromatography on a Dionex Ultimate 3000 nanoflow UPCL system (Thermo Scientific). Eluting peptides were directly analyzed by nanoelectrospray ionization-tandem mass spectrometry on a Thermo Orbitrap Elite (Thermo Scientific) instrument for a processing time of 1 h. Protein identification was provided by the

University of Texas at Austin Proteomics Facility following previously published procedures (Knauf et al., 2018). Scaffold (version Scaffold_4.3.4, Proteome Software Inc., Portland, OR) was used to validate MS/MS based peptide and protein identifications. Peptide identifications were accepted if they could be established at greater than 57.0% probability to achieve an FDR less than 0.5% by the Peptide Prophet algorithm (Keller et al., 2002) with Scaffold delta-mass correction. Protein identifications were accepted if they could be established at greater than 99.0% probability and contained at least 5 identified peptides. Protein probabilities were assigned by the Protein Prophet algorithm (Nesvizhskii et al., 2003). Proteins that contained similar peptides and could not be differentiated based on MS/MS analysis alone were grouped to satisfy the principles of parsimony. Proteins were annotated with GO terms from gene_association.goa_uniprot (downloaded Jul 14, 2014) (Ashburner et al., 2000).

2.10. TRiC/CCT substrate assay

This was adapted from a previously described assay (Won et al., 1998). Briefly, HEK293Ts were transfected with M72–3XFLAG, 24 h post transfection cells were lysed in NP-40 lysis buffer on ice for 20 min, clarified by centrifugation for 10 min and supernatants aliquoted into 4 parts. Samples were either mock treated or incubated with 15 mM EDTA or 5 mM $MgCl_2$ with or without 5 mM ATP for 40 min at room temperature. Samples were pre-cleared with normal Rabbit-IgG (Santa Cruz Biotech) and ProteinA/G PLUS-Agarose beads (Santa Cruz Biotech). Samples were immunoprecipitated using a mixture of 0.5 μg of rabbit anti-CCT8 antibody and 0.5 μg of rabbit TCP1 antibody and Protein A/G agarose beads overnight at 4 °C on an orbital rotator. Beads were boiled in SDS sample buffer at 95 °C for 10 min, resolved on 10% SDS-PAGE and immunoblotted.

2.11. In vitro transcription/translation

Assay was performed as previously described (Knowlton et al., 2018). Briefly, coupled *in vitro* transcription and translation reactions were conducted using the TNT coupled rabbit reticulocyte lysate (RRL) system (Promega, L4610) according to the manufacturer's instructions. All open reading frame templates for *in vitro* transcription and translation were sub-cloned into the pcDNA3.1+ vector. All reactions were incubated at 30 °C for variable intervals depending on the experimental conditions. Reactions were supplemented with [^{35}S]-methionine (Perkin Elmer, NEG709A500UC) for radiolabeling and RNasin Plus RNase Inhibitor (N2611). Translation reactions were terminated by four-fold dilution in stop buffer (20 mM HEPES-KOH, pH 7.4, 100 mM potassium acetate, 5 mM Magnesium acetate, 5 mM EDTA, 2 mM methionine, 1 mM DTT, 2 mM puromycin) unless otherwise specified. Samples were then resolved by native- and SDS-PAGE.

3. Results

3.1. M72 is not an active dUTPase

MCMV M72 is designated as a dUTPase homolog based on limited sequence similarity with other herpesviruses and homology to HCMV UL72 (Rawlinson et al., 1996). To determine whether M72 possesses intrinsic dUTPase activity, a previously described approach was employed (Leang et al., 2011). Briefly, transfected viral dUTPases and homologs were

purified from cell lysates and incubated with dUTP, where functional dUTPase enzymes convert dUTP to dUMP and pyrophosphate. The sample is then used in place of dTTP in a PCR reaction, where dUTP that has not been enzymatically processed will be incorporated into the amplicon and result in a successful reaction. MHV-68 ORF54 and its catalytic mutant, ORF54$^{H80A/D85N}$ (Leang et al., 2011), were used as positive and negative controls, respectively. Immunoblots confirmed expression and immunoprecipitation of transfected, epitope tagged M72 and ORF54 proteins (Fig. 1A). As expected, MHV-68 ORF54 showed enzymatic activity as a dUTPase, consuming dUTP in the *in vitro* reaction. The ORF54$^{H80A/D85N}$ catalytic mutant was incapable of depleting provided dUTP, resulting in a positive PCR reaction (Fig. 1B). In comparison to the controls, both amino- and carboxy-terminal epitope tagged M72 did not display dUTPase activity like the MHV68 ORF54 catalytic mutant (Fig. 1B). These results suggest that the MCMV M72 gene product is not an active dUTPase enzyme, likely playing an alternative role in virus infection.

3.2. Generation of M72 mutant viruses

To investigate the potential role of M72 in MCMV pathogenesis, the pARK25 bacterial artificial chromosome (BAC) containing the K181 (Perth) strain of MCMV (Redwood et al., 2005) was used to introduce two independent premature stop codons into the M72 open reading frame with established recombineering techniques (Upton et al., 2010). The schematic in Fig. 2A represents the mutagenesis strategy. Initially, a selection/counter selection cassette (sacB/Kan^R) was inserted into a region including the M72 open reading frame (corresponding to MCMV genome between nucleotide 102,772 and 105,791) by allelic exchange. This cassette was replaced in a second allelic exchange step with two independent amplicons containing engineered stop codons inserted within the M72 gene. The 5′-end of the M72 gene on the complementary strand is overlapped by the 5′ ends of M73 and M73.5 genes. To prevent disruption of M73 and M73.5, mutations were inserted into a non-overlapping region in the 5′ end of M72. The BACs were analyzed by restriction fragment length polymorphism (RFLP) and PCR/restriction digest to ensure the structural integrity and presence of intended mutations. Isolated BAC DNA digested with *HindIII* or *PstI* revealed the anticipated patterns due to the insertion of the sacB/Kan^R cassette. The M72.SK BAC digested with *HindIII* showed the appearance of a unique 2007 bp, while *PstI* digestion revealed the loss of a 4931 bp band and addition of a unique 8828 bp band. These differences were absent from the specific mutant BACs, which were indistinguishable from WT BAC (Fig. 2B). As expected, amplification of the region around M72 from WT and mutant BACs produced amplicons of 2082 bp, while the sacB/Kan^R containing M72.SK produced an amplicon of 4000 bp. Moreover, digestion of amplicons with *SpeI* or *NheI* revealed the insertion of specific mutations linked to each unique diagnostic restriction enzyme site in M72StopS and M72StopN (Fig. 2C), respectively. WT and mutant BAC DNAs were transfected into NIH3T3 fibroblasts and viruses recovered and amplified. No major differences in viral immediate-early (m123/IE1), early (m112–113/E1) or late (MCP/M86) proteins were seen in NIH3T3 cells infected with WT, M72StopS or M72StopN (Fig. 2D), suggesting that M72 likely does not influence viral protein expression during infection.

3.3. MCMV M72 augments viral replication in cell culture

To begin to understand the contribution of M72 to viral replication, the replication of M72StopS and M72StopN mutants were characterized in cell culture. In addition to murine fibroblasts, we assessed viral growth in endothelial and macrophage cell types, both of which are important to CMV infection. Analysis of yields during single-step infection (MOI = 5.0) showed that M72StopS and M72StopN mutants were attenuated by nearly 10-fold in murine fibroblasts (Fig. 3A) and endothelial cells (Fig. 3B) compared with WT virus. However, both the M72Stop mutant viruses replicated to comparable levels as the WT virus in a macrophage cell line (Fig. 3C) and BMDMs (Fig. 3D). Multi-step infection (MOI = 0.05) revealed similar trends in each of the three cell types; mutant viruses produced lower levels than WT virus in NIH3T3 and SVEC4–10 cells (Fig. 3E and F) and similar levels as WT virus in the macrophage cell line (Fig. 3G). Together these results indicate M72 augments virus replication in some cell types of cultured cells.

3.4. M72 contributes to early acute phase of infection in natural host

Since M72 plays a role in efficient replication in cell culture, we next sought to determine how disruption of M72 affects virus replication in the context of a natural host. BALB/cJ mice were infected *via* intraperitoneal (i.p.) inoculation with 10^5 PFU of the WT, M72StopS or M72StopN viruses, and viral loads in the spleen and salivary glands were determined. Compared with the WT virus, M72StopS and M72StopN viruses were each attenuated approximately 10-fold in spleens on day 3 post-inoculation (Fig. 4A). At day 5 post-inoculation, a similar trend was observed in infected spleens although with greater variation in titers, and differences between the loads of WT and M72Stop mutants did not reach statistical significance (Fig. 4B). Surprisingly, analysis of salivary gland titers at day 7 (Fig. 4C) and day 14 (Fig. 4D) post-inoculation demonstrated that the M72Stop mutants were present at similar levels as the WT virus. This finding indicates that the capacity of the M72Stop mutant viruses to disseminate in the natural host remains unaffected. Together, these data suggest that MCMV M72 contributes to acute replication of the virus during the early phase of infection, but is dispensable for dissemination in the natural host. Thus, this betaherpesvirus dUTPase homolog plays a role in viral pathogenesis.

3.5. Generation of tagged virus and evaluation of M72 protein expression

While introduction of premature translational stop codons into the predicted M72 ORF affected viral replication both *in vitro* and *in vivo*, little is known about M72. It is encoded in a transcriptionally complex region of the genome, and transcripts corresponding to the M72 gene have been detected in infected cells (Juranic Lisnic et al., 2013; Rapp et al., 1994; Scalzo et al., 2004). Moreover, peptides corresponding to M72 sequence have been detected in MCMV virions (Kattenhorn et al., 2004). However, the expression of M72 protein during infection has not been reported. Since M72-specific antibodies are not available, we engineered a recombinant virus in which a 3 × -FLAG epitope tag is appended to the carboxyl-terminus of M72. The predicted stop codon of M72 (nucleotides 103,083–103,086) of the K181 BAC was replaced with a sacB/Kan^R cassette *via* recombineering. In the subsequent step, this cassette was replaced with an amplicon containing a 3 × -FLAG epitope fused to the carboxyl-terminal end of M72 to generate MCMV M72.3XFlag (Fig.

5A). RFLP analysis (Fig. 5B), PCR amplification and sequencing (Fig. 5D) confirmed the presence of the inserted sequence, and infectious virus was recovered. To quantify the expression of M72 during infection, NIH3T3 fibroblasts were infected with M72.3XFlag at an MOI of 5 PFU/cell. Samples were harvested at the time of virus addition (t = 0) and at various intervals thereafter for immunoblot analyses. Expression of a ~ 46 kDa band, consistent with the estimated and observed molecular weight of full length, epitope tagged M72 (Fig. 1A), was observed as early as 6 h post infection (h.p.i.), reaching peak levels between 24 and 48 h.p.i. (Fig. 5C). Expression of immediate-early (m123/IE1), early (m112–113/E1) and late (gB/M55) gene products were observed as anticipated (Fig. 5C). Addition of the CMV DNA polymerase inhibitor phosphonoformic acid (PFA) at the time of infection did not interfere with the expression of IE1 or E1, but significantly reduced the expression of the late protein gB (Fig. 5C). M72 has previously been designated a late gene based on RNA expression (Scalzo et al., 2004). M72 protein expression was not adversely affected by the addition of PFA, but instead showed enhanced protein expression particularly for faster migrating isoforms of M72. Interestingly, additional, faster migrating protein bands were observed over the time course of infection. A similar pattern was observed upon detection of exogenously expressed FLAG-tagged M72 (Figs. 1A, 6B, and 7B), suggesting that the initial observation was not an artifact and that multiple M72 protein isoforms accumulate during infection. Based on the approximate molecular weights of the faster migrating isoforms, and the number and locations of multiple methionine residues in the N-terminus of M72, we hypothesized that initiation of M72 protein isoform expression could be initiated from internal methionine residues. A series of N-terminal truncations was constructed in which each methionine between M1 and M140 was used as the initiating methionine for the construct (Fig. 5E). Immunoblot analysis of NIH3T3 cells transfected with each of the N-terminal truncations was compared to MCMV-M72.3XFLAG infected cells run on the same gel. Virus infected cells showed the expected pattern of multiple M72 protein isoforms (Fig. 5F, left panel), and bands in infected cells migrated consistent with expression constructs encoding full length M72 (1–401), $M72^{(46–401)}$, $M72^{(76–401)}$ and $M72^{(139–401)}$ (Fig. 5F, right panel). Together, these results suggest a complex expression profile of M72 during infection.

3.6. Identifying interacting partners of M72

To begin to understand the function of M72, we sought to define cellular interacting protein partners of M72. M72–3XFlag or control plasmid were transfected into NIH3T3 fibroblasts. FLAG-immunoprecipitates were prepared, resolved by 10% SDS-PAGE and stained. Multiple bands were observed in the M72–3XFLAG sample relative to the vector control (Fig. 6A). A region of each lane in which multiple bands were differentially enriched, corresponding to approximately 55–70 kDa, were excised from each sample, subjected to in-gel tryptic digestion and LC-MS/MS analysis. Peptide sequences were compared to the UniProt mouse reference genome, and used to generate an initial list of 109 total unique proteins, excluding those of low confidence representation, low abundance, or those enriched in the control sample. Proteins for which a minimum of 10 peptide spectral matches in the experimental sample were detected, and those which showed at least a 2-fold enrichment over control samples were designated candidate interacting proteins (Table 1). Among the candidates meeting these criteria, all eight subunits of the TRiC/CCT complex

were significantly enriched in M72-containing immunoprecipitates. TRiC/CCT is a hetero-oligomeric complex that aids in cellular protein folding and assembly. It is a eukaryotic chaperonin and has eight paralogous subunits (TRiC/CCT 1–8) arranged in a stacked ring-like structure (Lopez et al., 2015). TRiC/CCT functions in an ATP-dependent manner and provides a physically defined compartment in which cellular protein domains or entire proteins can fold while being sequestered from the cytosol (Rüßmann et al., 2012). There are examples of TRiC/CCT complex interacting with viral proteins like EBNA-3 protein of EBV (Kashuba et al., 1999), hepatitis C virus NS5B (Inoue et al., 2011), influenza PB2 (Fislová et al., 2010), rabies virus N and P proteins (Zhang et al., 2013), and reovirus σ3 capsid protein (Knowlton et al., 2018), indicating that it is an important cellular factor across diverse groups of viruses.

3.7. M72 is a substrate of the TRiC/CCT complex

To validate the results of the MS experiment, M72–3XFLAG and each of the HA-tagged CCT 1–8 subunits were transiently co-expressed in HEK293T cells. Immunoprecipitation followed by immunoblotting revealed that M72 co-immunoprecipitated each of the co-transfected subunits of TRiC/CCT complex, except CCT5 (Fig. 6B). Interestingly, CCT5 was consistently and reproducibly expressed to significantly lower levels when co-transfected with M72. Whether this represents an artifact of co-expression, or is indicative of an antagonism remains unclear. Thus, we are unable to conclusively confirm the interaction between M72 and CCT5 observed by mass spectrometry (Table 1). An irrelevant, comparably sized and epitope-tagged protein, Lsm14a, did not co-immunoprecipitate with M72 indicating the interaction was specific. Similar findings were made using M72 with an epitope tag appended to the amino- (data not shown) terminus (Fig. 6B), indicating that the epitope tag did not influence the interaction.

Since the TRiC/CCT complex is an interacting partner with M72 and required for homeostatic protein folding of many cellular proteins, such as actin (Gao et al., 1992), we thought that M72 might modulate TRiC/CCT complex activity. However, infection of cells with WT, M72StopS, or M72StopN viruses showed no discernable differences or changes of expression of individual CCT proteins, and actin protein levels remained constant throughout each infection condition (data not shown). This finding suggested that M72 does not affect the expression or activity of the TRiC/CCT complex during MCMV infection and raises the possibility that M72 is a client protein of the TRiC/CCT complex.

To determine whether M72 is a substrate of the TRiC/CCT complex, we employed a previously reported CCT substrate assay (Won et al., 1998). TRiC/CCT substrates should be released from the complex in the presence of $MgCl_2$ and ATP, but remain associated when treated with a divalent cation chelator, such as EDTA. Thus, to assess the effect of these treatments on M72 release from isolated TRiC/CCT complex, cell lysates were prepared from M72–3XFLAG-transfected HEK293T cells, and divided into four equal aliquots. Aliquots were incubated with either EDTA, $MgCl_2$ or, $MgCl_2$ with ATP for 40 min at room temperature. Samples were then immunoprecipitated with a mixture of anti-CCT1 and CCT8 antibodies to isolate TRiC/CCT complexes and their associated substrates, and separated by SDS-PAGE. Immunoblotting for M72 revealed a substantial decrease in M72

co-precipitated with TRiC/CCT complexes in the presence of $MgCl_2$ and ATP, while comparable levels of M72 were observed in mock- and EDTA-treated samples (Fig. 6C). This result confirms the interaction of M72 with the TRiC/CCT complex and suggests that M72 is dissociated from the complex in an ATP-dependent manner.

To more directly test whether M72 is a TRiC/CCT substrate, we investigated the association of *in vitro* translated M72 with TRiC/CCT over time in rabbit reticulocyte lysates (RRLs). RRLs are a common tool used to identify and characterize TRiC/CCT substrates (Freund et al., 2014; Kasembeli et al., 2014), including human β-actin (Gao et al., 1992) and reovirus σ3 (Knowlton et al., 2018). Actin (an obligate TRiC/CCT substrate), GFP (which does not require TRiC/CCT to fold) or M72 were translated *in vitro* in the presence of S^{35}-labled methionine for 5, 10, or 20 min. Reactions were resolved on parallel native- and SDS-PAGE gels. As anticipated (Knowlton et al., 2018), newly translated actin was observed in association with a large complex (> 750 kDa) in native gels, corresponding to the actin/TRiC complex (Gao et al., 1992; Kasembeli et al., 2014; Knowlton et al., 2018). Over the time course, a low molecular weight (< 60 kDa) form of actin accumulated, consistent with the release of monomeric actin from TRiC/CCT (Fig. 6D). GFP, which is not a TRiC/CCT substrate, did not form a high molecular weight complex with TRiC/CCT, and instead consistently accumulated in a monomeric state during translation. In comparison, nascent M72 migrated in a high molecular weight complex with TRiC (Fig. 6D). However, native M72 did not accumulate as a free monomer consistent with its migration on a denaturing gel (Fig. 6E), but instead showed a diffuse band ranging from approximately 100 to 150 kDa, suggesting that M72 forms an oligomer.

To determine whether M72 forms an oligomer, full-length and C-terminal truncations of M72–3XFLAG (Fig. 7A) were co-transfected with GFP-M72 into HEK293T cells. Immunoprecipitation followed by immunoblotting revealed that GFP-M72 co-immunoprecipitates with full length M72–3XFLAG, suggesting that M72 forms homo-oligomers both *in vitro* (Fig. 6D) and *in vivo* (Fig. 7B). Binding of M72–3XFLAG to GFP-M72 is relatively comparable upon deletion of the C-terminus to amino acid 283, but is markedly diminished for $M72^{(1–253)}$ and $M72^{(1–226)}$. While formally possible the diminished binding $M72^{(1–226)}$ and $M72^{(1–253)}$ is due to modest expression, it is worth noting that they are expressed as well as $M72^{(1–339)}$, $M72^{(1–311)}$, and $M72^{(1–282)}$, yet consistently co-IP less GPF-M72, suggesting that the region of M72 encompassing aa 227–283 are important for efficient oligomerization. $M72^{(1–199)}$ co-precipitates with GFP-M72 as well as full length M72, but this binding is substantially reduced for $M72^{(1–172)}$ and $M72^{(1–136)}$, and is completely lost for the smallest fragment, $M72^{(1–107)}$. Together, these results indicate that regions of M72 from aa 173–200 and aa 227–283 contribute to M72 oligomerization. To determine whether the ability of M72 mutants to oligomerize correlates with association of M72 with the TRiC/CCT complex, full-length and a subset of C-terminal truncations of M72–3XFLAG (Fig. 7A) were co-transfected with HA-CCT8 into HEK293T cells. Immunoprecipitation followed by immunoblotting confirmed that full length M72–3XFLAG could co-IP CCT8, and $M72^{(1–199)}$ could co-IP similar amounts of CCT8 as WT (Fig. 7C). It also revealed that $M72^{(1–311)}$, which showed a higher level of oligomerization (Fig. 7B), also precipitated more CCT8 than WT M72. Similarly, M72 mutants defective for oligomerization were similarly, diminished in their capacity to co-IP CCT8. Together, these

data indicate that M72 forms homo-oligomers (Fig. 7B) which correlates with its ability to associate with components of the TRiC/CCT complex (Fig. 7C).

4. Discussion

In this study, we provide an initial characterization of the role of MCMV M72 gene during infection *in vitro* and *in vivo*. Although related to herpesvirus dUTPase enzymes, we confirm that M72 does not possess intrinsic enzymatic activity (Fig. 1), and likely plays no direct role in supporting nucleotide biogenesis during infection. Genetic disruption unveiled a function for M72 in virus replication in fibroblast and endothelial cell lines in culture (Figs. 2 and 3). In addition, M72 promotes acute virus replication in the early stage of infection in a natural host (Fig. 4A). Interestingly, mutation of M72 had little effect on the capacity of MCMV to disseminate to the salivary glands of infected animals (Fig. 4C and D). M72 protein is expressed as early as 6 h.p.i. with increasing levels up to 48 h. Additional, faster migrating M72 isoforms are also detected and accumulate throughout infection (Fig. 5C). We find that M72 associates with, and is a substrate of, the eukaryotic TRiC/CCT chaperonin complex (Fig. 6). Like other well characterized TRiC/CCT substrates, such as actin (Gao et al., 1992), M72 forms oligomers or higher-order aggregates *in vitro* and *in vivo*. This interaction is mediated by a bipartite region of the central portion of M72. While the specific function of M72 during infection remains unclear, our results indicate complex viral and host regulation of M72 protein expression during infection, and demonstrate that M72 contributes to MCMV replication and pathogenesis.

dUTPases are classified into three subgroups based on their oligomerization states: monomeric, dimeric and trimeric. Avian and mammalian herpesvirus dUTPase enzymes are exclusively monomeric, and bioinformatics analysis suggest that trimeric and monomeric dUTPases contain five conserved motifs for catalytic activity (John et al., 2001). Herpesvirus dUTPases also have an additional motif 6 of unknown function (Baldo and McClure, 1999; Davison and Stow, 2005; John et al., 2001). MCMV M72 was designated as a dUTPase homolog based on limited sequence similarity and positional homology with other herpesvirus dUTPases (Rawlinson et al., 1996). Among human beta herpesvirus dUTPase homologs, HCMV UL72 and Human Herpesvirus 6A (HHV-6A) U45 are catalytically inactive (Ariza et al., 2014; Caposio et al., 2004). Our results confirm that, like other betaherpesvirus dUTPase homologs, M72 is not a functional enzyme (Fig. 1). Moreover, an examination of the M72 protein sequence shows that it lacks the 5 motifs necessary for enzymatic activity and only has the herpesvirus conserved motif 6 (Davison and Stow, 2005). While many other herpesvirus dUTPases also fulfill enzyme-independent roles (Ariza et al., 2009, 2013; Leang et al., 2011; Madrid and Ganem, 2012), our results indicate that M72 plays an exclusively alternate role during infection.

Previous functional profiling studies of the entire HCMV genome indicated that HCMV UL72 is non-essential for replication (Dunn et al., 2003; Yu et al., 2003), and a UL72 mutant removing the entire open reading frame (Caposio et al., 2004) has a modest replication defect in cell culture. Our examination of MCMV M72 mutant infection revealed that M72 contributes to virus replication in murine fibroblasts and endothelial cells, similar to the results for HCMV UL72. These results are consistent at both high and low multiplicities of

infection (Fig. 3A, B, E, and F)), suggesting that the defect is MOI-independent. However, we also observed that M72 mutant viruses produced yields comparable to, or even higher than, WT MCMV in murine macrophage cell lines (Fig. 3C and G) and BMDMs (Fig. 3D). This result may be indicative of a tissue specific contribution of M72 during viral infection.

In the context of a natural host, the MHV-68 dUTPase, ORF54, is required for establishment of latency but dispensable for acute replication in lungs of infected mice (Leang et al., 2011). Additionally, pseudorabies virus lacking its dUTPase homolog, UL50, is also attenuated for virulence and replication in infected swine (Jons et al., 1997). However, there are no reports of the contribution of betaherpesvirus designated dUTPase homologs to infection in the natural host. We show here that M72 augments virus replication during acute replication in spleen at early times post infection (Fig. 4). Interestingly, M72Stop mutants effectively disseminated to the salivary glands of infected animals, like WT virus (Fig. 4C and D). Thus, despite early acute defects in replication seen *in vivo* (Fig. 4A), M72-deficient viruses can infect and replicate in the disseminating cell population, showing no defects at later times post infection. Mononuclear phagocytes are the main cell type that contributes to dissemination of MCMV (Stoddart et al., 1994), likely after acquiring virus from susceptible cells at sites of primary infection. This result is consistent with our findings in cell culture where there is a modest defect in viral replication in endothelial cells and fibroblasts, but no impairment in the capacity of these viruses to infect and grow in macrophage/monocytes cells (Fig. 3). While not an essential gene, M72 appears to alleviate barriers to replication in some types of cells. Future studies will provide insights into the host restriction mechanisms overcome by M72.

HCMV UL72 and MCMV M72 have been classified as late gene product (Caposio et al., 2004; Scalzo et al., 2004) based on northern blot analyses. However, using an epitope-tagged virus, we observe M72 protein expression as early as 6 h.p.i. and this expression is unaffected by addition of PFA (Fig. 5C). By comparison, we observed diminished expression of glycoprotein B/M55, a late gene, in the presence of PFA, indicating that drug treatment was effective. The expression pattern of M72 protein more closely mimics that of the m112/3 (E1) protein, a well know delayed-early gene. Thus, M72 is likely a leaky-late gene product, requiring delayed early protein function, but not requiring viral DNA replication.

Another unanticipated result was the observation of faster migrating FLAG-epitope tagged species by SDS-PAGE analysis from cells infected with MCMV-M72.3XFlag. A similar expression profile, including the faster migrating bands, was observed in infected murine endothelial (SVEC) and macrophage (RAW264.7) cell lines (data not shown), suggesting this phenomenon is independent of cell type. An additional independent HA-epitope tagged M72 recombinant virus displays similar faster migrating bands (data not shown), indicating these bands are not an artifact of the FLAG epitope tag. Initial investigations suggest that that these faster migrating M72 protein isoforms are similar in size to proteins translated from internal methionine positions within the M72 annotated ORF. HCMV UL136 is expressed as multiple protein isoforms and a detailed characterization of the different isoforms using independent recombinant viruses revealed novel functions for each (Caviness et al., 2016, 2014; Umashankar et al., 2011). These isoforms are produced by a complex

transcriptional program that uses distinct transcription initiation sites for each isoform (Caviness et al., 2014). The M72-M75 region of the MCMV genome is transcriptionally complex (Juranic Lisnic et al., 2013; Scalzo et al., 2004). However, there do not appear to be distinct transcriptional start sites or alternative splicing for the M72 transcript. We also observe multiple M72 proteins isoforms being expressed following transfection of plasmids encoding the M72 ORF (Figs. 1A, 6B, and 7B), indicating that this is not a function of viral infection or replication. M72StopS and M72StopN mutants we report would be predicted to interrupt some, but not all of the protein isoforms observed by western blot analysis. M72StopS and M72StopN would be predicted to terminate translation between the 3rd and 4th methionine within the ORF. Thus, the full length and two largest possible isoforms would be interrupted by these mutations. However, it is formally possible that additional downstream ORFs remain open and could be expressed during infection. We show that interruption of M72 by the –StopS and –StopN mutations are sufficient to impair viral replication *in vitro* and *in vivo*, indicating that longest isoforms of M72 interrupted by both mutations have important functions during infection.

Previous attempts to identify interacting partners of MCMV proteins using a yeast two-hybrid screen showed that M72 engages multiple other viral proteins (Fossum et al., 2009). Since there are no reports of host factors that interact with M72, we used a proteomics approach to identify cellular proteins that bind M72. Identification of such proteins my provide clues to M72 function. We identified and confirmed the interaction of M72 *in vitro* and *in vivo* with components of the eukaryotic TRiC/CCT complex (Fig. 5). TRiC/CCT is a well characterized eukaryotic chaperonin and contributes to protein folding of an estimated 5–10% of the cellular proteome (Yam et al., 2008). Our original LC-MS/MS analysis identified all 8 subunits of the TRiC/CCT complex co-precipitating with M72 expressed in in NIH3T3 cells(Table 1). We repeatedly observed that transfected M72–3XFLAG was incapable of co-immunoprecipitating CCT5/ε in HEK293T cells. Whether this is an artifact of overexpression or indicative of a cell line difference, is unclear. There are multiple examples of viruses engaging this complex, including EBV (Kashuba et al., 1999), influenza virus (Fislová et al., 2010), rabies virus (Zhang et al., 2013), and reovirus ((Knowlton et al., 2018)). Our experiments provide evidence that MCMV M72 is likely another viral client of the TRiC/CCT complex (Fig. 6). There is no consensus sequence recognition recognized for TRiC/CCT client proteins. However, some biochemical features, such as β-sheets content, aggregation propensity and formation of higher-order complexes are associated with TRiC/CCT binding (Yam et al., 2008). While little information is available about the structure of M72, previous bioinformatics studies (Davison and Stow, 2005), as well as initial bioinformatics analysis using structure prediction tools, suggest the presence of multiple β-sheets in M72. Moreover, our data indicate that M72 is capable of forming higher-order oligomers or aggregates (Figs. 6D and 7B), and this feature correlates with M72's ability to associate with CCT subunits (Fig. 7C), further supporting M72 as a substrate of the TRiC/CCT complex. Since M72 augments virus replication and is not an essential MCMV gene, identification of other MCMV (and HCMV) essential gene products as TRiC/CCT clients may provide the rationale for development of TRiC/CCT inhibitors as potential antiviral compounds.

In this report, we characterized the previously unexplored MCMV protein M72. Previous studies have established roles for other designated dUTPase genes among herpesviruses, and future efforts will focus on identifying the specific molecular mechanism of M72 function during infection. It will be important to determine whether the multiple detected isoforms of M72 protein have distinct functions during infection and how each contributes to pathogenesis. It will also be critical to continue confirming and characterizing host proteins we have identified as candidate M72-interacting proteins, which we anticipate will provide insight into the specific function of M72 during MCMV infection.

Acknowledgements

We thank Ren Sun and Ting-Ting Wu (the University of California at Los Angeles) for the kind gift of MHV-68 ORF54 WT and its catalytic mutant, Dr. Kyong-Tai Kim and Dohyun Lee (Pohang University of Science and Technology, Republic of Korea) for HA-tagged CCT expression constructs, and Dr. Laura Hanson (Texas Women's University, Denton, TX) for antibody. We also thank Dr. Chris Sullivan and laboratory, Dr. Bryan Davies, and Dr. Ian Molineux (UT Austin) for useful discussion and editorial feedback.

Funding

This work supported by startup funds provided by the University of Texas at Austin, Cancer Prevention and Research Institute of Texas (CPRIT – R1202), and Public Health Service awards AI032539, AI122563, GM007347. The funders had no role in study design, data collection and interpretation, or the decision to submit the work for publication.

References

Ariza ME, Rivailler P, Glaser R, Chen M, Williams MV, 2013 Epstein-barr virus encoded dUTPase containing exosomes modulate innate and adaptive immune responses in human dendritic cells and peripheral blood mononuclear cells. PLoS One 8, e69827. [PubMed: 23894549]

Ariza ME, Glaser R, Williams MV, 2014 Human herpesviruses-encoded dUTPases: a family of proteins that modulate dendritic cell function and innate immunity. Front. Microbiol 5.

Ariza M-E, Glaser R, Kaumaya PTP, Jones C, Williams MV, 2009 The EBV-encoded dUTPase activates NF-κB through the TLR2 and MyD88-dependent signaling pathway. J. Immunol 182, 851–859. [PubMed: 19124728]

Ashburner M, Ball CA, Blake JA, Botstein D, Butler H, Cherry JM, Davis AP, Dolinski K, Dwight SS, Eppig JT, Harris MA, Hill DP, Issel-Tarver L, Kasarskis A, Lewis S, Matese JC, Richardson JE, Ringwald M, Rubin GM, Sherlock G, 2000 Gene ontology: tool for the unification of biology. The gene ontology consortium. Nat. Genet 25, 25–29. [PubMed: 10802651]

Baldo AM, McClure MA, 1999 Evolution and horizontal transfer of dUTPase-encoding genes in viruses and their hosts. J. Virol 73, 7710–7721. [PubMed: 10438861]

Barry PA, Lockridge KM, Salamat S, Tinling SP, Yue Y, Zhou SS, Gospe JSM, Britt WJ, Tarantal AF, 2006 Nonhuman primate models of intrauterine cytomegalovirus infection. ILAR J 47, 49–64. [PubMed: 16391431]

Boppana SB, Ross SA, Fowler KB, 2013 Congenital cytomegalovirus infection: clinical outcome. Clin. Infect. Dis 57, S178–S181. [PubMed: 24257422]

Caposio P, Riera L, Hahn G, Landolfo S, Gribaudo G, 2004 Evidence that the human cytomegalovirus 46-kDa UL72 protein is not an active dUTPase but a late protein dispensable for replication in fibroblasts. Virology 325, 264–276. [PubMed: 15246266]

Caviness K, Cicchini L, Rak M, Umashankar M, Goodrum F, 2014 Complex expression of the UL136 gene of human cytomegalovirus results in multiple protein isoforms with unique roles in replication. J. Virol 88, 14412–14425. [PubMed: 25297993]

Caviness K, Bughio F, Crawford LB, Streblow DN, Nelson JA, Caposio P, Goodrum F, 2016 Complex interplay of the UL136 isoforms balances cytomegalovirus replication and latency. mBio 7.

Datta S, Costantino N, Court DL, 2006 A set of recombineering plasmids for gram-negative bacteria. Gene 379, 109–115. [PubMed: 16750601]

Davison AJ, Stow ND, 2005 New genes from old: redeployment of dUTPase by herpesviruses. J. Virol 79, 12880–12892. [PubMed: 16188990]

Dunn W, Chou C, Li H, Hai R, Patterson D, Stolc V, Zhu H, Liu F, 2003 Functional profiling of a human cytomegalovirus genome. Proc. Natl. Acad. Sci 100, 14223. [PubMed: 14623981]

Fislová T, Thomas B, Graef KM, Fodor E, 2010 Association of the influenza virus RNA polymerase subunit PB2 with the host chaperonin CCT. J. Virol 84, 8691–8699. [PubMed: 20573828]

Fossum E, Friedel CC, Rajagopala SV, Titz B, Baiker A, Schmidt T, Kraus T, Stellberger T, Rutenberg C, Suthram S, Bandyopadhyay S, Rose D, von Brunn A, Uhlmann M, Zeretzke C, Dong Y-A, Boulet H, Koegl M, Bailer SM, Koszinowski U, Ideker T, Uetz P, Zimmer R, Haas J, 2009 Evolutionarily conserved herpesviral protein interaction networks. PLoS Pathog 5, e1000570. [PubMed: 19730696]

Freund A, Zhong FL, Venteicher AS, Meng Z, Veenstra TD, Frydman J, Artandi SE, 2014 Proteostatic control of telomerase function through TRiC-mediated folding of TCAB1. Cell 159, 1389–1403. [PubMed: 25467444]

Gao Y, Thomas JO, Chow RL, Lee G-H, Cowan NJ, 1992 A cytoplasmic chaperonin that catalyzes β-actin folding. Cell 69, 1043–1050. [PubMed: 1351421]

Griffiths PD, 2012 Burden of disease associated with human cytomegalovirus and prospects for elimination by universal immunisation. Lancet Infect. Dis 12, 790–798. [PubMed: 23017365]

Hizi A, Herzig E, 2015 dUTPase: the frequently overlooked enzyme encoded by many retroviruses. Retrovirology 12, 70. [PubMed: 26259899]

Inoue Y, Aizaki H, Hara H, Matsuda M, Ando T, Shimoji T, Murakami K, Masaki T, Shoji I, Homma S, Matsuura Y, Miyamura T, Wakita T, Suzuki T, 2011 Chaperonin TRiC/CCT participates in replication of hepatitis C virus genome via interaction with the viral NS5B protein. Virology 410, 38–47. [PubMed: 21093005]

John EM, Nigel WD, Duncan JM, 2001 Evolution of the dUTPase gene of mammalian and avian Herpesviruses. Curr. Protein Pept. Sci 2, 325–333. [PubMed: 12369929]

Jons A, Gerdts V, Lange E, Kaden V, Mettenleiter TC, 1997 Attenuation of dUTPase-deficient pseudorabies virus for the natural host. Vet. Microbiol 56, 47–54. [PubMed: 9228681]

Juranic Lisnic V, Babic Cac M, Lisnic B, Trsan T, Mefferd A, Das Mukhopadhyay C, Cook CH, Jonjic S, Trgovcich J, 2013 Dual analysis of the murine cytomegalovirus and host cell transcriptomes reveal new aspects of the virus-host cell interface. PLoS Pathog 9, e1003611. [PubMed: 24086132]

Kaiser WJ, Sridharan H, Huang C, Mandal P, Upton JW, Gough PJ, Sehon CA, Marquis RW, Bertin J, Mocarski ES, 2013 Toll-like receptor 3-mediated necrosis via TRIF, RIP3, and MLKL. J. Biol. Chem 288, 31268–31279. [PubMed: 24019532]

Kasembeli M, Lau WC, Roh SH, Eckols TK, Frydman J, Chiu W, Tweardy DJ, 2014 Modulation of STAT3 folding and function by TRiC/CCT chaperonin. PLoS Biol 12, e1001844. [PubMed: 24756126]

Kashuba E, Pokrovskaja K, Klein G, Szekely L, 1999 Epstein-Barr virus-encoded nuclear protein EBNA-3 interacts with the epsilon-subunit of the T-complex protein 1 chaperonin complex. J. Hum. Virol 2, 33–37. [PubMed: 10200597]

Kattenhorn LM, Mills R, Wagner M, Lomsadze A, Makeev V, Borodovsky M, Ploegh HL, Kessler BM, 2004 Identification of proteins associated with murine cytomegalovirus virions. J. Virol 78, 11187–11197. [PubMed: 15452238]

Keller A, Nesvizhskii AI, Kolker E, Aebersold R, 2002 Empirical statistical model to estimate the accuracy of peptide identifications made by MS/MS and database search. Anal. Chem 74, 5383–5392. [PubMed: 12403597]

Kim S, Park D-Y, Lee D, Kim W, Jeong Y-H, Lee J, Chung S-K, Ha H, Choi B-H, Kim K-T, 2014 Vaccinia-related kinase 2 mediates accumulation of polyglutamine aggregates via negative regulation of the chaperonin TRiC. Mol. Cell. Biol 34, 643–652. [PubMed: 24298020]

Knauf GA, Cunningham AL, Kazi MI, Riddington IM, Crofts AA, Cattoir V, Trent MS, Davies BW, 2018 Exploring the antimicrobial action of quaternary amines against Acinetobacter baumannii. mBio 9.

Knowlton JJ, de Castro Fernández, Ashbrook I, Gestaut AW, Zamora DR, Bauer PF, Forrest JA, Frydman JC, Risco J, Dermody C, T.S., 2018 The TRiC chaperonin controls reovirus replication through outer-capsid folding. Nat. Microbiol 3, 481–493. [PubMed: 29531365]

Leang RS, Wu T-T, Hwang S, Liang LT, Tong L, Truong JT, Sun R, 2011 The anti-interferon activity of conserved viral dUTPase ORF54 is essential for an effective MHV-68 infection. PLoS Pathog 7, e1002292. [PubMed: 21998588]

Lerner DL, Wagaman PC, Phillips TR, Prospero-Garcia O, Henriksen SJ, Fox HS, Bloom FE, Elder JH, 1995 Increased mutation frequency of feline immunodeficiency virus lacking functional deoxyuridine-triphosphatase. Proc. Natl. Acad. Sci 92, 7480–7484. [PubMed: 7638216]

Lopez T, Dalton K, Frydman J, 2015 The mechanism and function of group II chaperonins. J. Mol. Biol 427, 2919–2930. [PubMed: 25936650]

Madrid AS, Ganem D, 2012 Kaposi's sarcoma-associated herpesvirus ORF54/dUTPase downregulates a ligand for the NK activating receptor NKp44. J. Virol 86, 8693–8704. [PubMed: 22674989]

Mocarski E Jr, 2007 Betaherpes viral genes and their functions. In: Arvin A, Campadelli-Fiume G, Mocarski E, Moore PS, Roizman B, Whitley R, Yamanishi K (Eds.), Human Herpesviruses: Biology, Therapy, and Immunoprophylaxis Cambridge University Press, Cambridge.

Nesvizhskii AI, Keller A, Kolker E, Aebersold R, 2003 A statistical model for identifying proteins by tandem mass spectrometry. Anal. Chem 75, 4646–4658. [PubMed: 14632076]

Plosa EJ, Esbenshade JC, Fuller MP, Weitkamp J-H, 2012 Cytomegalovirus infection. Pediatr. Rev 33, 156–163. [PubMed: 22474112]

Pyles RB, Sawtell NM, Thompson RL, 1992 Herpes simplex virus type 1 dUTPase mutants are attenuated for neurovirulence, neuroinvasiveness, and reactivation from latency. J. Virol 66, 6706–6713. [PubMed: 1328686]

Ramanan P, Razonable RR, 2013 Cytomegalovirus infections in solid organ transplantation: a review. Infect. Chemother 45, 260–271. [PubMed: 24396627]

Rapp M, Lučin P, Messerle M, Loh LC, Koszinowski UH, 1994 Expression of the murine cytomegalovirus glycoprotein H by recombinant vaccinia virus. J. Gen. Virol 75, 183–188. [PubMed: 8113726]

Rawlinson WD, Farrell HE, Barrell BG, 1996 Analysis of the complete DNA sequence of murine cytomegalovirus. J. Virol 70, 8833–8849. [PubMed: 8971012]

Redwood AJ, Messerle M, Harvey NL, Hardy CM, Koszinowski UH, Lawson MA, Shellam GR, 2005 Use of a murine cytomegalovirus K181-derived bacterial artificial chromosome as a vaccine vector for immunocontraception. J. Virol 79, 2998–3008. [PubMed: 15709020]

Ross J, Williams M, Cohen JI, 1997 Disruption of the varicella–zoster virus dUTPase and the adjacent ORF9A gene results in impaired growth and reduced syncytia formationin vitro. Virology 234, 186–195. [PubMed: 9268149]

Rüßmann F, Stemp MJ, Mönkemeyer L, Etchells SA, Bracher A, Hartl FU, 2012 Folding of large multidomain proteins by partial encapsulation in the chaperonin TRiC/CCT. Proc. Natl. Acad. Sci 109, 21208–21215. [PubMed: 23197838]

Scalzo AA, Dallas PB, Forbes CA, Mikosza ASJ, Fleming P, Lathbury LJ, Lyons PA, Laferté S, Craggs MM, Loh LC, 2004 The murine cytomegalovirus M73.5 gene, a member of a 3′ co-terminal alternatively spliced gene family, encodes the gp24 virion glycoprotein. Virology 329, 234–250. [PubMed: 15518804]

Schleiss MR, 2006 Nonprimate models of congenital cytomegalovirus (CMV) infection: gaining insight into pathogenesis and prevention of disease in newborns. ILAR J 47, 65–72. [PubMed: 16391432]

Stoddart CA, Cardin RD, Boname JM, Manning WC, Abenes GB, Mocarski ES, 1994 Peripheral blood mononuclear phagocytes mediate dissemination of murine cytomegalovirus. J. Virol 68, 6243–6253. [PubMed: 8083964]

Stratton KR, Durch JS, Lawrence RS (Eds.), 2000 Vaccines for the 21st Century: A Tool for Decisionmaking The National Academies Press, Washington, DC.

Umashankar M, Petrucelli A, Cicchini L, Caposio P, Kreklywich CN, Rak M, Bughio F, Goldman DC, Hamlin KL, Nelson JA, Fleming WH, Streblow DN, Goodrum F, 2011 A novel human cytomegalovirus locus modulates cell type-specific outcomes of infection. PLoS Pathog 7, e1002444. [PubMed: 22241980]

Upton JW, Kaiser WJ, Mocarski ES, 2010 Virus inhibition of RIP3-dependent necrosis. Cell Host Microbe 7, 302–313. [PubMed: 20413098]

Ward TM, Williams MV, Traina-Dorge V, Gray WL, 2009 The simian varicella virus uracil DNA glycosylase and dUTPase genes are expressed in vivo, but are non-essential for replication in cell culture. Virus Res 142, 78–84. [PubMed: 19200445]

Won K-A, Schumacher RJ, Farr GW, Horwich AL, Reed SI, 1998 Maturation of human Cyclin E requires the function of eukaryotic chaperonin CCT. Mol. Cell. Biol 18, 7584–7589. [PubMed: 9819444]

Yam AY, Xia Y, Jill Lin H-T, Burlingame A, Gerstein M, Frydman J, 2008 Defining the TRiC/CCT interactome links chaperonin function to stabilization of newly-made proteins with complex topologies. Nat. Struct. Mol. Biol 15, 1255–1262. [PubMed: 19011634]

Yu D, Silva MC, Shenk T, 2003 Functional map of human cytomegalovirus AD169 defined by global mutational analysis. Proc. Natl. Acad. ScI 100, 12396. [PubMed: 14519856]

Zhang J, Wu X, Zan J, Wu Y, Ye C, Ruan X, Zhou J, 2013 Cellular chaperonin CCTγ contributes to rabies virus replication during infection. J. Virol 87, 7608–7621. [PubMed: 23637400]

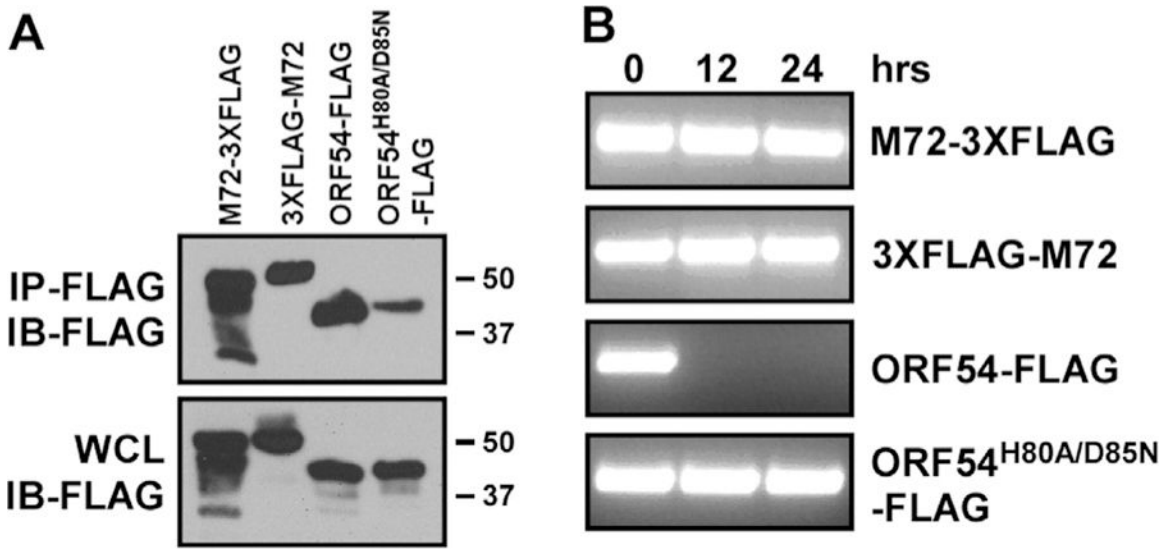

Fig. 1.

M72 is not an active dUTPase. A) Immunoblot (IB) analysis of immunoprecipitations (IP) and whole cell lysates (WCL) from HEK293Ts transfected 24 h with the indicated expression vector. B) Ethidium bromide (EtBr) stained agarose gel of PCR reactions utilizing individual dNTPs, with dTTP replaced by dUTP following incubation with IPs from (A). Presence of a PCR product indicates intact dUTP, and a non-functional dUTPase homolog.

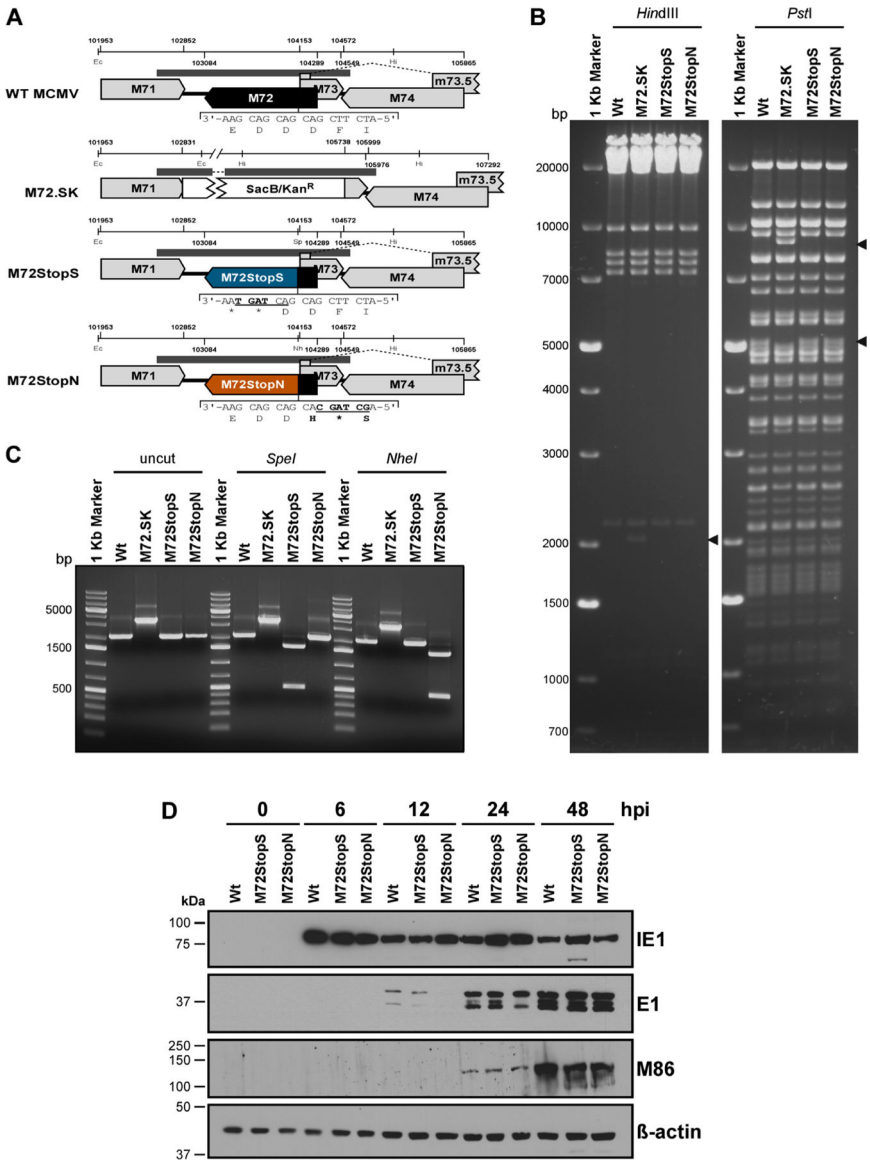

Fig. 2.

Generation of M72StopS and M72StopN recombinant viruses. A) Schematic diagram of genomic location of M72 and mutagenesis strategy to generate M72StopS and M72StopN. Numbers represent MCMV genomic coordinates (GenBank Accession number AM886412.1), and abbreviations indicate restriction enzyme sites (Hi, *HindIII*; Ec, *EcoRI*; Sp, *SpeI*; Nh, *NheI*). M72StopS and M72StopN were generated by a two-step allelic exchange strategy (see Materials & Methods) inserting, and then replacing, a selection/counterselection cassette (SacB/Kan^R). Nucleotide and amino acids changed are indicated in bold, and underlined sequences represent introduced diagnostic restriction enzyme sites. Grey bars represent diagnostic PCR amplicons in C). B) RFLP analysis of WT, M72.SK, M72StopS and M72StopN BACs. Isolated DNA was digested with the indicated enzyme, separated on a 0.6% agarose gel and visualized by EtBr staining. Arrowheads indicate specific important DNA fragments addressed in Results. C) Infectious virion DNA from the

indicated viruses was isolated, and amplicons from the M72 locus generated by PCR. Amplicons were digested with the indicated enzyme or left uncut. Products were separated on a 1.0% agarose gel and visualized by EtBr staining. D) IB analysis of MCMV IE1, E1, M86 and β-actin expression in NIH3T3 cells infected 0–48 h with the indicated virus (MOI = 5.0).

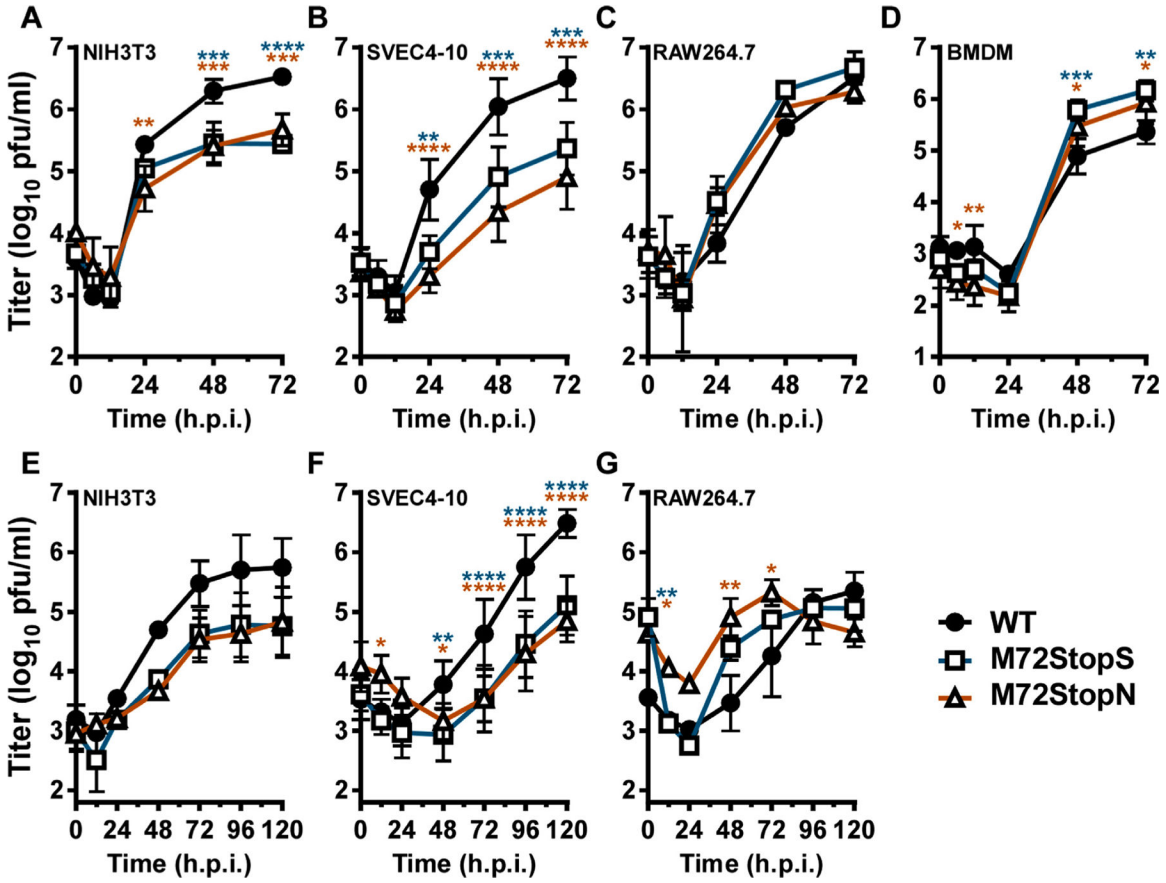

Fig. 3.

MCMV M72 augments virus replication in cell culture. (A–D) Single-step (5 PFU/cell) and (E–G) Multi-step (0.05 PFU/cell) growth curves in NIH3T3 fibroblasts (A and D), SVEC4–10 endothelial cells (B and E), RAW264.7 macrophages (C and F), and bone marrow derived macrophages (D) infected with WT, M72StopS or M72StopN recombinant viruses. Each data point represents n = 3–6 replicates. Error bars represent standard deviation. Statistical analysis at each time point was performed using two-way ANOVA analysis with a Tukey's multiple comparison test. *p < 0.01, ** – p < 0.001, *** – p < 0.0001, **** – P < 0.00001. Color of asterisks denotes the statistical difference of each mutant from WT. The 0 h. time points represent the time immediately post wash and addition of fresh complete media. h.p.i.; hours post infection.

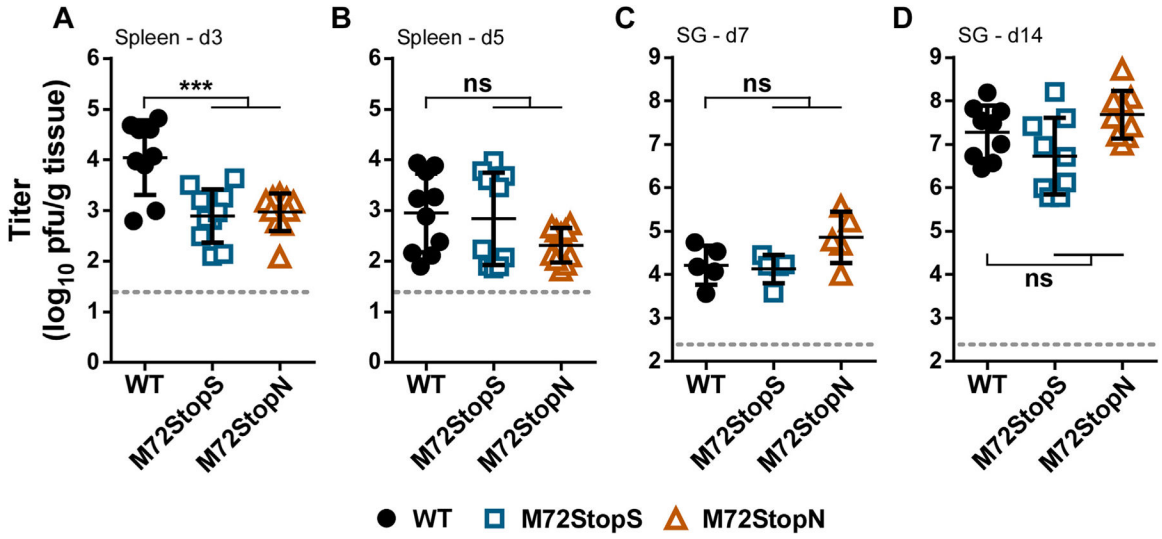

Fig. 4.

MCMV M72 augments virus replication in the early phase of acute infection in the natural host. (A–D) Organ titers from BALB/cJ mice infected with 10^5 PFU of either WT, M72StopS or M72StopN viruses. Spleen (A–B) and salivary gland (C–D) were collected at the indicated day (d) post infection, and infection virus determined by plaque assay on NIH3T3 fibroblasts. Each time point represents n = 10–15 mice per group. Error bars represent standard deviation. Statistical analysis at each time point was performed using two-way ANOVA analysis with a Tukey's multiple comparison test. *** – $p < 0.0001$, ns – not significant.

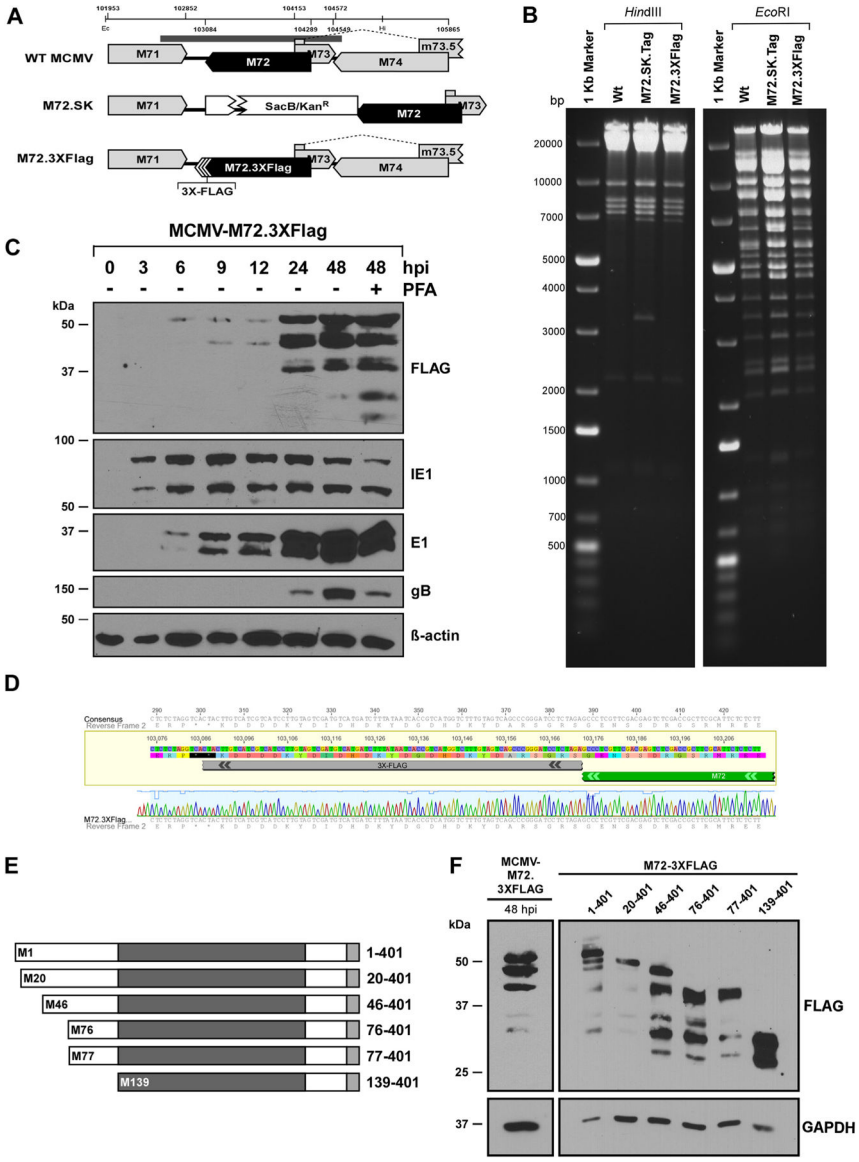

Fig. 5.

Expression of M72 protein during infection. A) Schematic diagram of genomic location of M72 and mutagenesis strategy to generate M72.3XFlag. Numbers represent MCMV genomic coordinates (GenBank Accession number AM886412.1), and abbreviations indicate restriction enzyme sites (Hi, *HindIII*; Ec, *EcoRI*). M72.3XFlag was generated by a two-step allelic exchange strategy (see Materials & Methods) inserting, and then replacing, a selection/counterselection cassette (SacB/Kan^R) with a 3XFLAG epitope tag. B) RFLP analysis of WT, M72.SK.Tag, and M72.3XFlag BACs. Isolated DNA was digested with the indicated enzyme, separated on a 0.6% agarose gel and visualized by EtBr staining. C) Immunoblot for FLAG, IE1, E1, gB and actin from whole cell lysates of NIH3T3 cells infected (MOI=5.0) MCMV M72.3XFlag virus in the presence or absence of 200 μg/ml PFA. Samples were collected at the indicated time points post infection, separated by SDS-PAGE and western blot analysis. The 0 h. time point represents the time of addition of virus

to the dishes. D) Representative results of sequencing and alignment of M72.3XFlag insertion site. Amplicons were generated from viral genomic DNA using primers flanking the end of M72. E) Schematic diagram of epitope-tagged M72 N-terminal mutants initiating from specific methionine residues within the open reading frame. Numbers preceded by “M” denote the amino acid position of the internal methionine for initiation of protein expression for each mutant. Dark Grey box indicates putative ‘dUTPase’ domain. Light grey box indicates 3XFlag epitope tag. Numbers denote amino acid numbers. F) Immunoblot analysis for FLAG and GAPDH of NIH3T3 cells transfected with the indicated N-terminal FLAG-tagged M72 construct, or infected with MCMV-M72.3XFlag.

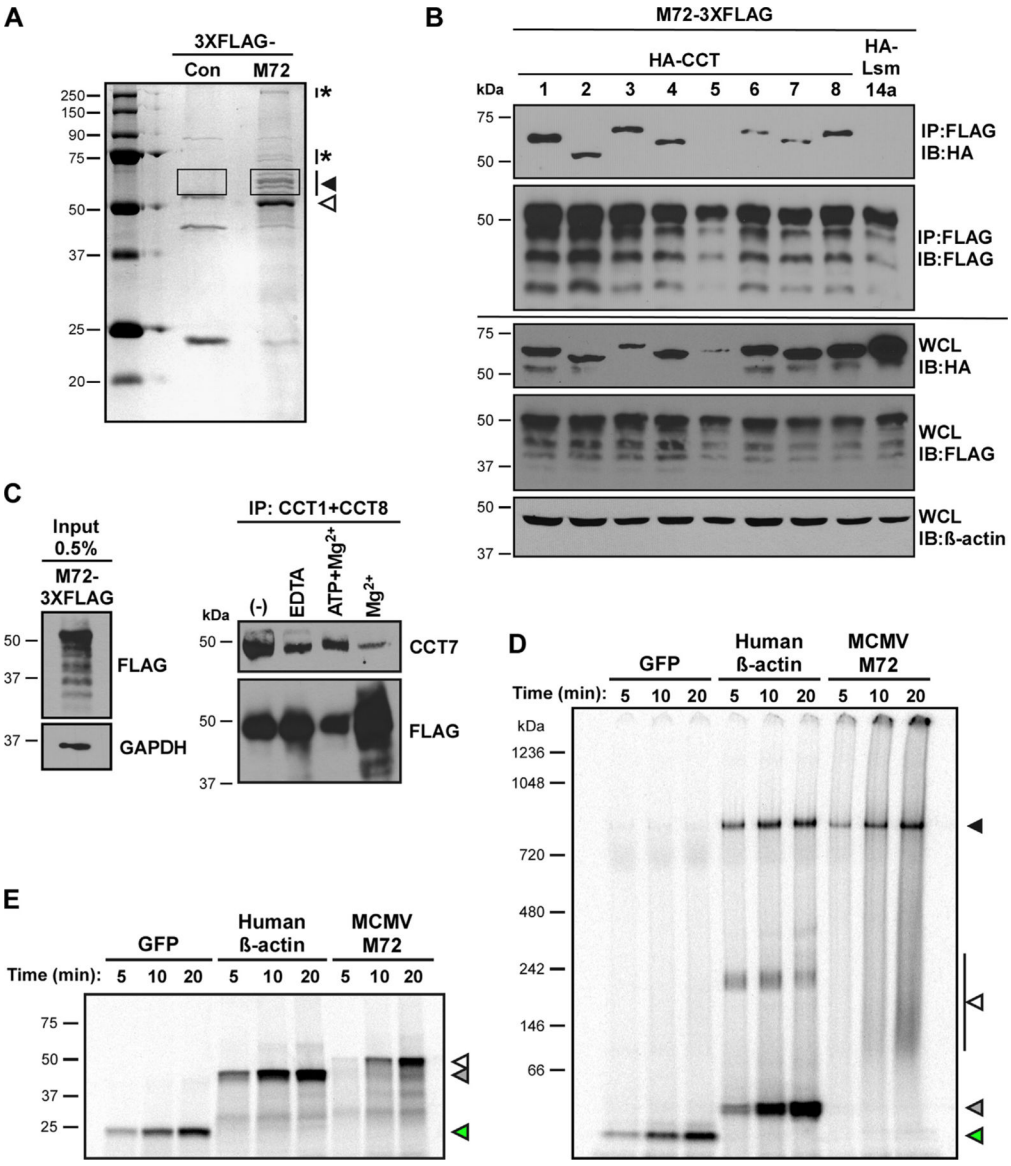

Fig. 6.

M72 associates with and is a substrate of the TRIC/CCT complex. A) Coomassie stained SDS-PAGE gel of FLAG-immunoprecipitates from NIH3T3 fibroblasts transfected with M72–3XFLAG or empty vector control (Con). White arrow indicates M72–3XFLAG. Black arrowhead and boxed region denote region of differentially enriched bands excised and further analyzed by LC-MS/MS (Table 1). Asterisks indicate additional regions of potential differentially enrich proteins. B) IB analysis for HA, FLAG, and actin in IP and WCL from HEK293Ts co-transfected with M72–3XFLAG and HA-epitope tagged TRiC/CCT or control as indicated. C) IB analysis for CCT7 and FLAG from TRiC/CCT substrate assay. HEK293Ts were transfected with M72–3XFLAG, whole cell lysates collected, aliquoted into 4 parts and incubated with EDTA, $MgCl_2$ with or without ATP, or mock treated. Aliquots were subjected to IP with a mixture of TCP1/CCT1 and CCT8 antibodies, separated on SDS-PAGE gel and immunoblotted with the indicated antibodies. D-E) Native

(D) and SDS- (E) PAGE of ^{35}S-methionine (Met)-labelled green fluorescent protein (GFP), β-actin, and MCMV M72 translated for the intervals shown in rabbit reticulocyte lysates (RRLs). Green arrow indicates GFP, grey arrow indicates actin, white arrow indicates M72, and black arrow indicates TRiC/CCT associated proteins.

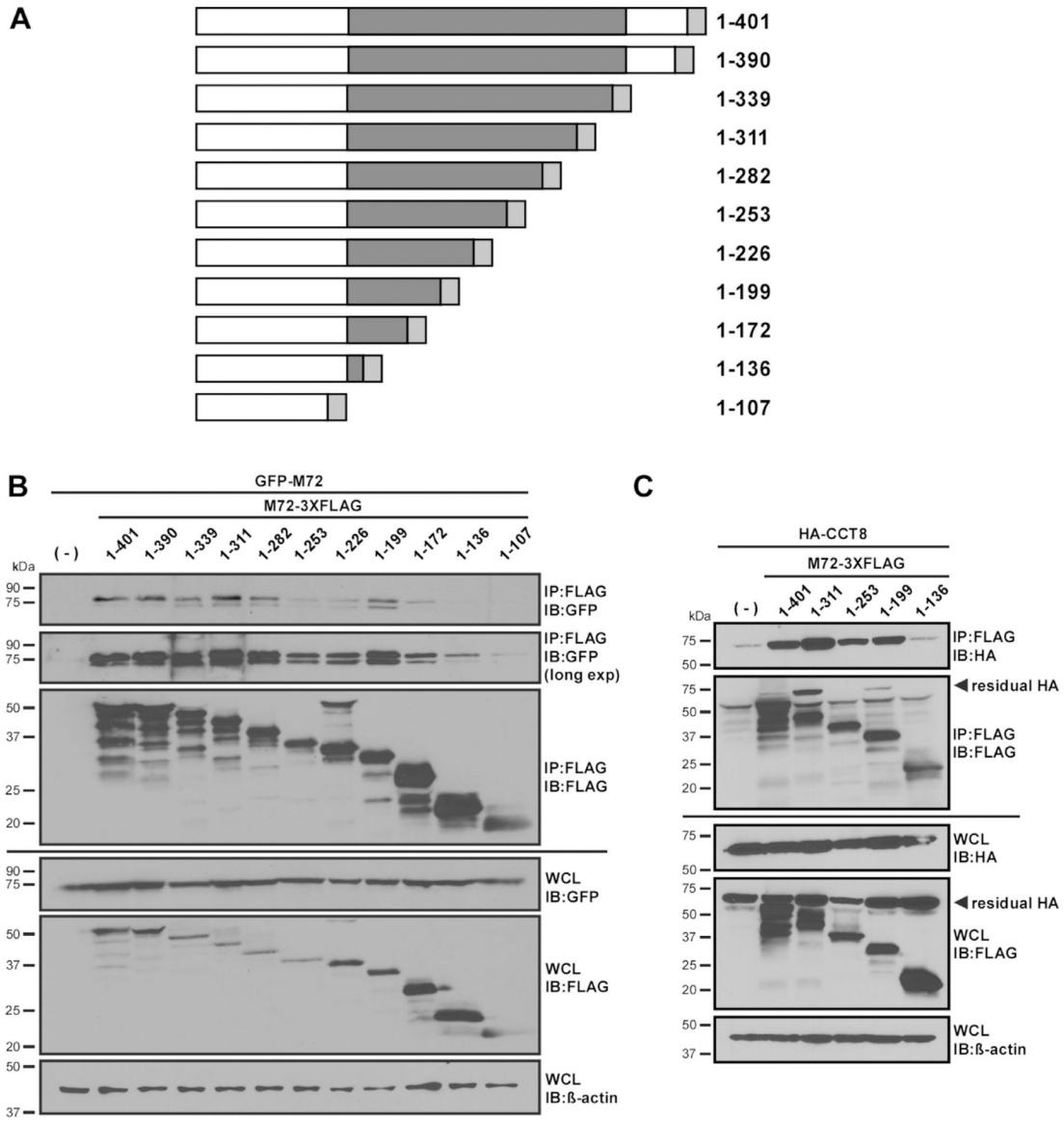

Fig. 7.

M72 forms self-associating oligomers in cell culture. A) Schematic diagram of epitope-tagged M72 carboxy-terminal truncation mutants. Dark Grey box indicates putative 'dUTPase' domain. Light grey box indicates 3XFlag epitope tag. Numbers denote amino acid numbers. B) IB analysis for FLAG, GFP, and actin in IP and WCL from NIH3T3 fibroblasts co-transfected with eGFP-M72 and the indicated 3XFlag-tagged M72 plasmids. C) IB analysis for FLAG, HA, and actin in IP and WCL from HEK293Ts co-transfected with HA-CCT8 and the indicated 3XFlag-tagged M72 plasmids.

Table 1

Candidate M72-interacting cellular proteins identified by mass spectrometry.

Identified protein	UNIPROT Accession	kDa	Peptide spectral counts (PSM)		Fold enrichment
			Con	M72-	
T-complex protein 1 subunit epsilon (Cct5)	TCPE_MOUSE	60	2	151	75.5
T-complex protein 1 subunit eta (Cct7)	TCPH_MOUSE	60	2	150	75.0
tRNA-splicing ligase RtcB homolog	RTCB_MOUSE	55	1	39	39.0
T-complex protein 1 subunit beta (Cct2)	TCPB_MOUSE	57	4	149	37.3
T-complex protein 1 subunit zeta (Cct6a)	TCPZ_MOUSE	58	3	110	36.7
T-complex protein 1 subunit delta (Cct4)	TCPD_MOUSE	58	5	144	28.8
T-complex protein 1 subunit theta (Cct8)	TCPQ_MOUSE	60	8	174	21.8
T-complex protein 1 subunit alpha (Tcp1)	TCPA_MOUSE	61	11	142	12.9
Polymerase I and transcript release factor	PTRF_MOUSE	44	2	15	7.5
T-complex protein 1 subunit gamma (Cct3)	TCPG_MOUSE	61	0	169	–
60 S ribosomal protein L4	RL4_MOUSE	61	0	38	–
CCR4-NOT transcription complex subunit 2	CNOT2_MOUSE	60	0	34	–
CCR4-NOT transcription complex subunit 6-like	CNO6L_MOUSE	63	0	18	–
Heterogeneous nuclear ribonucleoprotein K	B2M1R6_MOUSE	49	0	17	–
Protein FAM98A	FA98A_MOUSE	55	0	14	–
Nucleolin	NUCL_MOUSE	77	0	13	–
Protein disulfide-isomerase	PDIA1_MOUSE	57	0	12	–
26 S protease regulatory subunit 4	PRS4_MOUSE	49	0	11	–
Isoform 3 of Myelin expression factor 2	MYEF2_MOUSE	63	0	11	–
Heterogeneous nuclear ribonucleoprotein L	G5E924_MOUSE	67	0	10	–